Electronic Supplementary Material (ESI) for Materials Advances.

# Supporting Information for

## A facile, green and scalable approach to fabricate hierarchical ZnAl-LDH for efficient removal of hexavalent chromium

Tingting Liu[a], Meiqi Zheng[a], Kaiyue Ji[d], Xiaomeng Xue[a], Jiangrong Yang[a], Mingfei Shao[a], Haohong Duan*[b,d], Xianggui Kong*[a,c]

a State Key Laboratory of Chemical Resource Engineering, Beijing University of Chemical Technology, Beijing, 100029, China.

b Qingyuan Innovation Laboratory, Quanzhou, 362801, China.

c Quzhou Institute for Innovation in Resource Chemical Engineering, Zhejiang, China

d Department of Chemistry, Tsinghua University, Beijing, China

* Corresponding author:

E-mail: hhduan@mail.tsinghua.edu.cn (H. Duan); kongxg@mail.buct.edu.cn (X. Kong)

## Table of Content

# 1.Experimental section

## 1.1 Preparation of ZnAl-LDH-D

ZnAl-LDH-D was synthesized as follows: Firstly, 0.04 mol of ZnO and 0.02 mol of $Al(NO_3)_3 \cdot 9H_2O$ were dispersed into 100 mL of distilled water separately. Then, the suspension of ZnO and the solution of $Al(NO_3)_3$ were simultaneously pumped into the colloid mill reactor with rotating at 2000 rpm at room temperature. Subsequently, the mixture slurry was ageing at 25 °C for 2 hours followed by washing with deionized water and dry in oven. The ZnAl-LDH-D was finally obtained.

To obtain the intermediate samples from reaction system in early reaction stage, the sample was instantly separated at desired contact time and dispersed in extensive anhydrous ethanol, and then collected the samples by centrifugation.

## 1.2 Characterization of Materials

The crystal structure of resulting sample was analyzed by a powder X-ray diffraction device (JDX-3530, Tokyo, Japan) using Cu Kα radiation ($\lambda$=1.5418Å) with a $2\theta$ value ranging from 5° to 70° with a scanning speed of $10° \text{ min}^{-1}$. Solid state NMR spectroscopy was carried out using Bruker Avance III 400MHz WB. Microscopic morphology and dispersion of all elements of substances were characterized using scanning electron microscopy (SEM, Merlin VP Compact, 15 kV) and transmission electron microscope (TEM; JEOL-2010, 200 kV). Energy-dispersive spectroscopy (EDS) mapping was recorded on Tecnai F20. The chemical bonds and functional groups of ZnAl-LDH were determined using the Fourier Transform Infrared Spectroscopy (FTIR) of JASCO FTIR-670 Plus (Tokyo, Japan) with a resolution of 4 $cm^{-1}$ and a scan time =16 in transmission mode. Samples are prepared using the KBr method. The nitrogen adsorption and desorption isotherms of the samples were measured using a Micromeritics ASAP 2020 instrument (Norcross, Georgia, USA), and the specific surface area and pore structure were calculated by the BET method and the Barrett-Joyner-Halenda (BJH) model. The valence band positions of samples were measured by X-rayphotoelectron spectroscopy (XPS) (ESCA 5800; ULV AC-PHI, Inc., Kanagawa, Japan) using a monochromated Al Kα X-ray source at 200 W. The data analysis was conducted using XPS peak software (version 2.3.12.8).

## 1.3 Adsorption Experiments

All the adsorption experiments were carried out at 25 °C. Adsorption performance of ZnAl-LDH-D to heavy metals was evaluated with a series of Cr(VI) concentrations (10, 20, 50, 100, and 200 mg/L) with $K_2Cr_2O_4$ as pollutant. The dosage of ZnAl-LDH-D was 0.05 g with solution volume of 50 ml. The resulting mixture was stirred for a desired adsorption time and separated with a 0.22 μm membrane filter. The concentrations of Cr(VI) in aqueous solution were determined by inductively coupled plasma optical emission spectrometry (ICP-7500, Shimadzu Co, Japan). The adsorption capacity (*qt*) of heavy metal ions was calculated according to the following equation:

$$q_t = \frac{(c_0 - c_t)V}{m}$$

where $C_0$ (mg/L) is the initial concentrationsof Cr (mg/L); $C_t$ corresponding the concentration of Cr in solution at time of t (mg/L); V is the volume of solution (L); and m is the mass of the adsorbent (g).

In the case of evaluating the initial pH value on the adsorption performance to Cr(VI), the pH values of the Cr(VI) solutions were adjusted from 4.0 to 10.0 that was adjusted by $HNO_3$ or NaOH solution. For the selectivity evaluation, the initial concentration of Cr (VI) was set to 60 mg/L and the concentration of competitive anions was set to 60 mg/L, in which the NaCl, $NaNO_3$, $Na_2SO_4$ and $Na_2CO_3$ were used as anions source.

## 2. Supplemental Figures and Tables

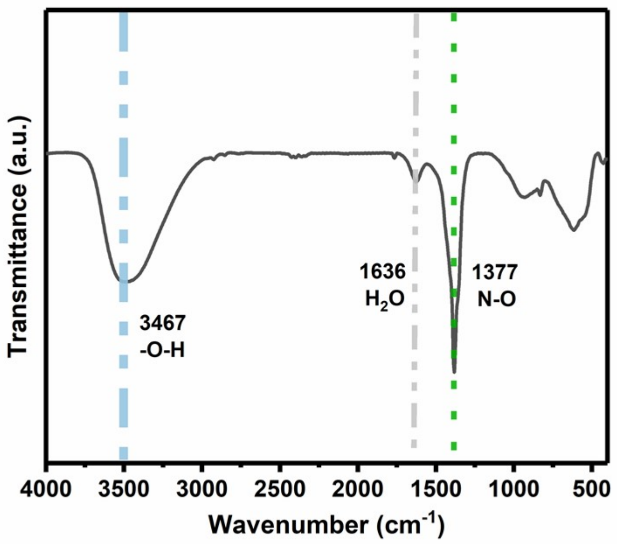

**Fig. S1** FITR spectra of ZnAl-LDH-D.

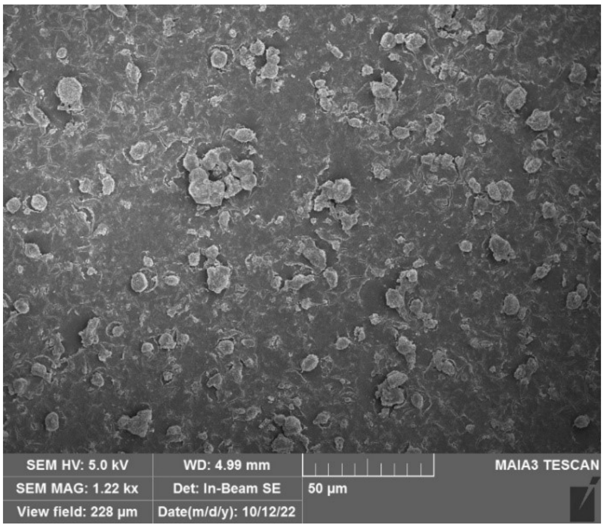

**Fig. S2** SEM image of ZnAl-LDH-D.

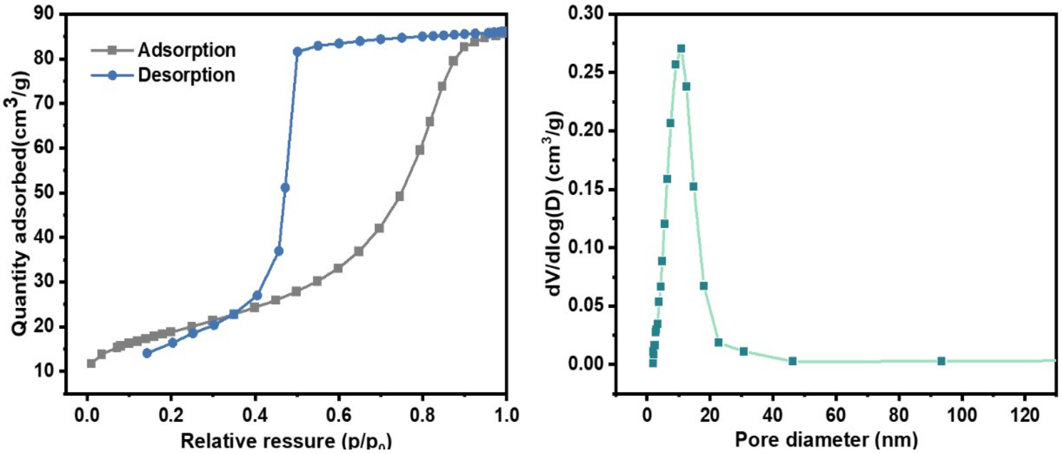

**Fig. S3** The $N_2$ adsorption-desorption isotherm and the pore size distributions of ZnAl-LDH-D.

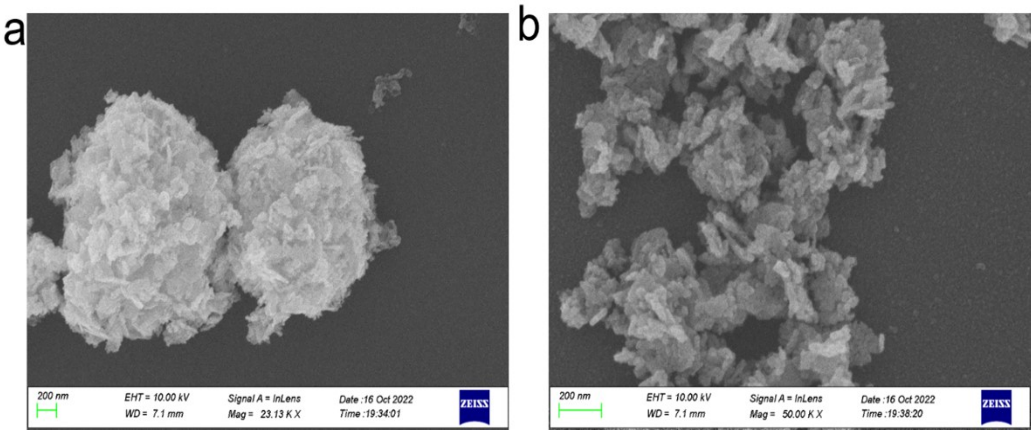

**Fig. S4** The SEM images of original ZnO.

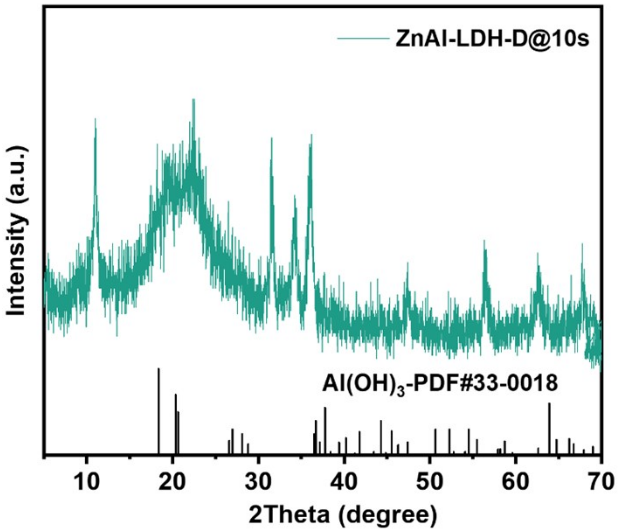

**Fig. S5** The XRD pattern sample obtained at less 10 second.

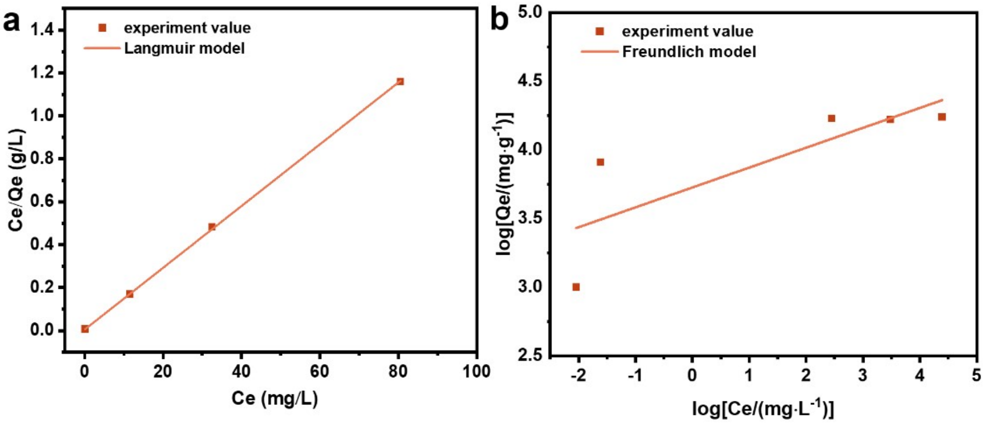

**Fig. S6** (a) The Langmuir adsorption isotherm plots and (b) The Freundlich adsorption isotherm plots for the adsorption of Cr(VI).

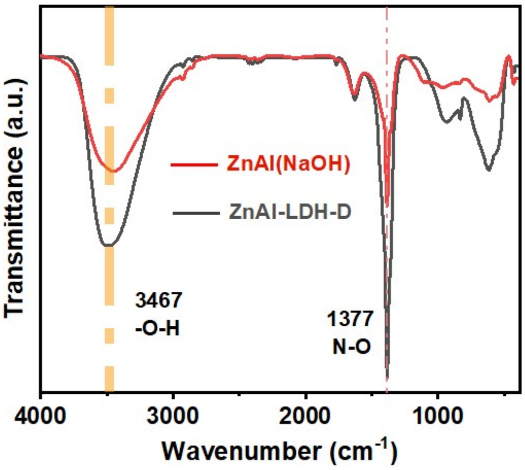

**Fig. S7** FITR spectra of ZnAl-LDH-D and ZnAl-LDH synthesized by NaOH, $Zn(NO_3)_2$ and

$Al(NO_3)_3$.

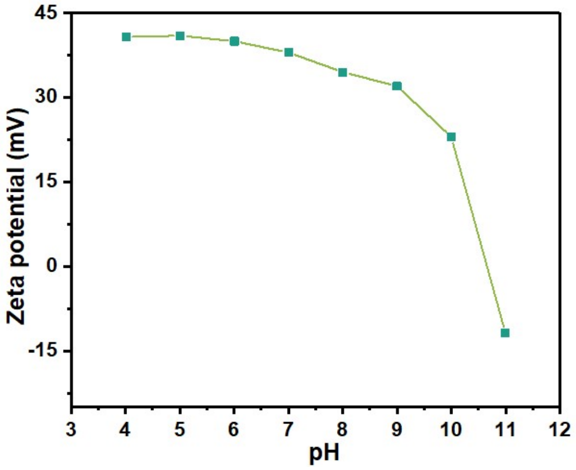

**Fig.S8** Zeta potentials of ZnAl-LDH-D.

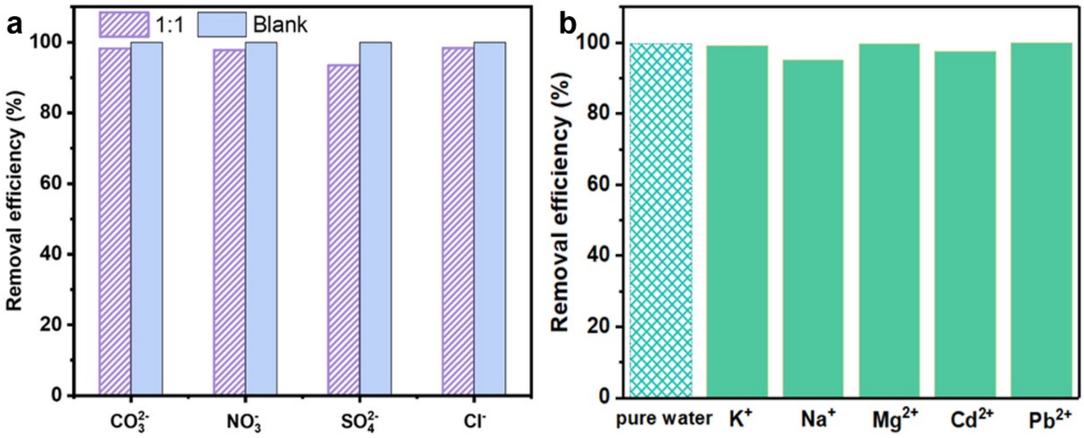

**Fig. S9**. (a) Effect of the co-existing anions on $Cr^{VI}$ removal with ZnAl-LDH-D, in which all the concentration of anions and $Cr^{VI}$ was 60 mg/L (dose = 0.1 g/L, t=2 h); (b) Effect of the co-existing cations on $Cr^{VI}$ removal with ZnAl-LDH-D, in which all the concentration of cations was 300 mg/L with $Cr^{VI}$ was 60 mg/L. (dose = 0.1 g/L, t=2 h).

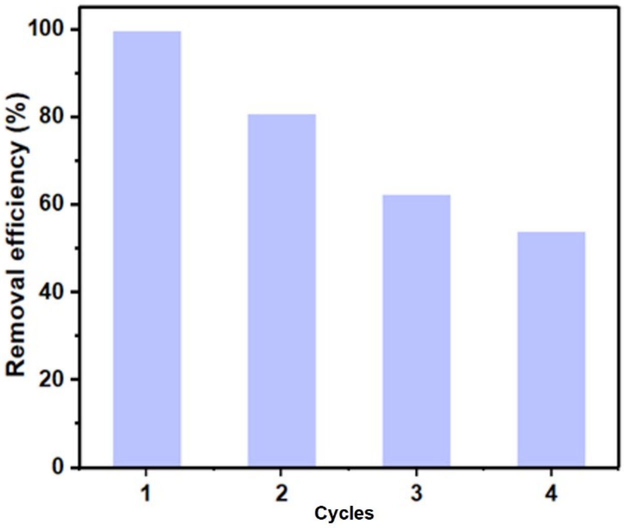

**Fig. S10** Recycling use of ZnAl-LDH-D for adsorption of $Cr^{VI}$.

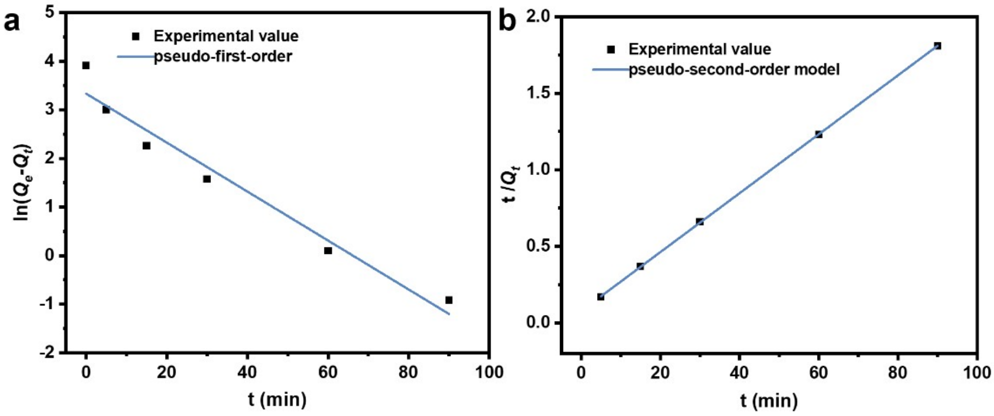

**Fig. S11** The kinetics plots of ZnAl-LDH-D for the adsorption of $Cr^{VI}$: (a) Pseudo-first-order model; (b) Pseudo-second-order model.

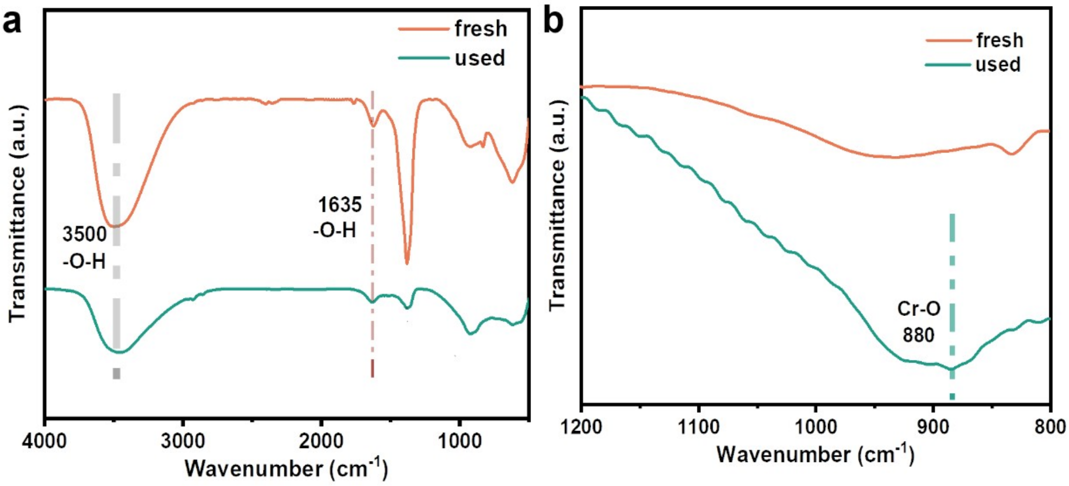

**Fig. S12** FTIR spectrums of ZnAl-LDH-D before and after removal of $Cr^{VI}$.

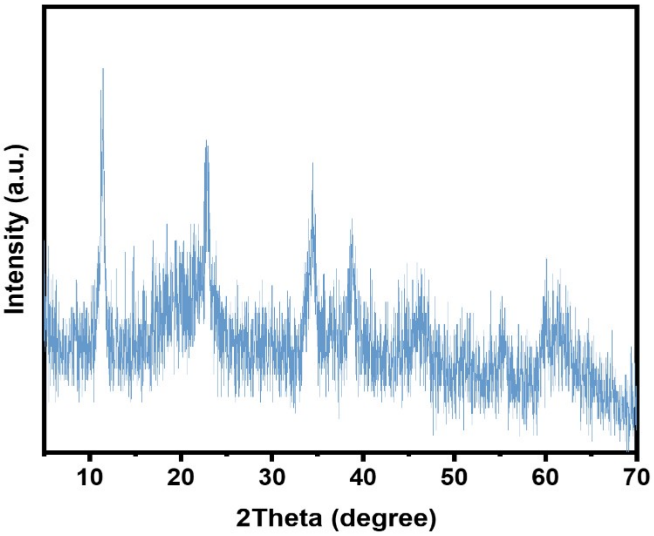

**Fig. S13** The XRD pattern of ZnAl-LDH-D with $D_2O$ instead of $H_2O$ in the synthesis process.

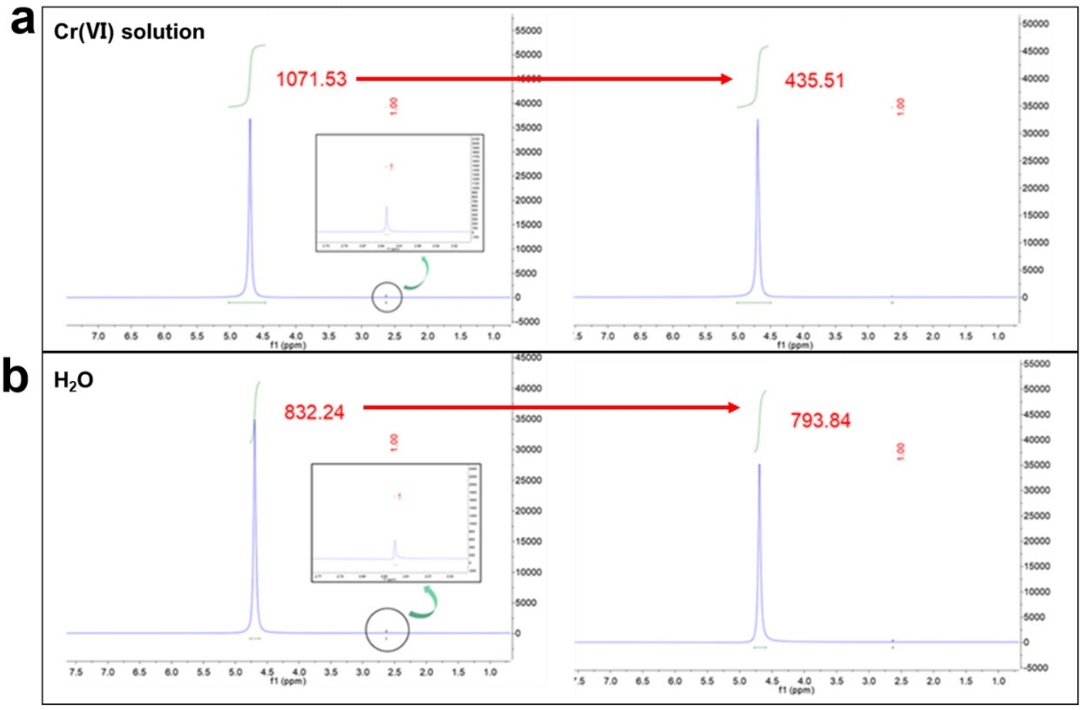

**Fig. S14** (a) $^1H$ NMR spectra of $Cr^{VI}$ solution before and after adsorption; (b) Control experiments in water solution.

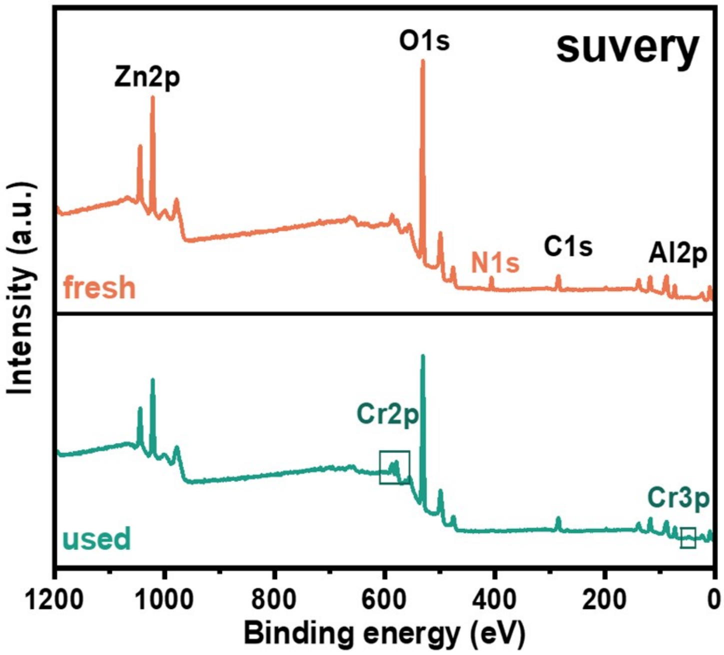

**Fig.** S15 XPS survey spectra of ZnAl-LDH before and after removal of $Cr^{VI}$.

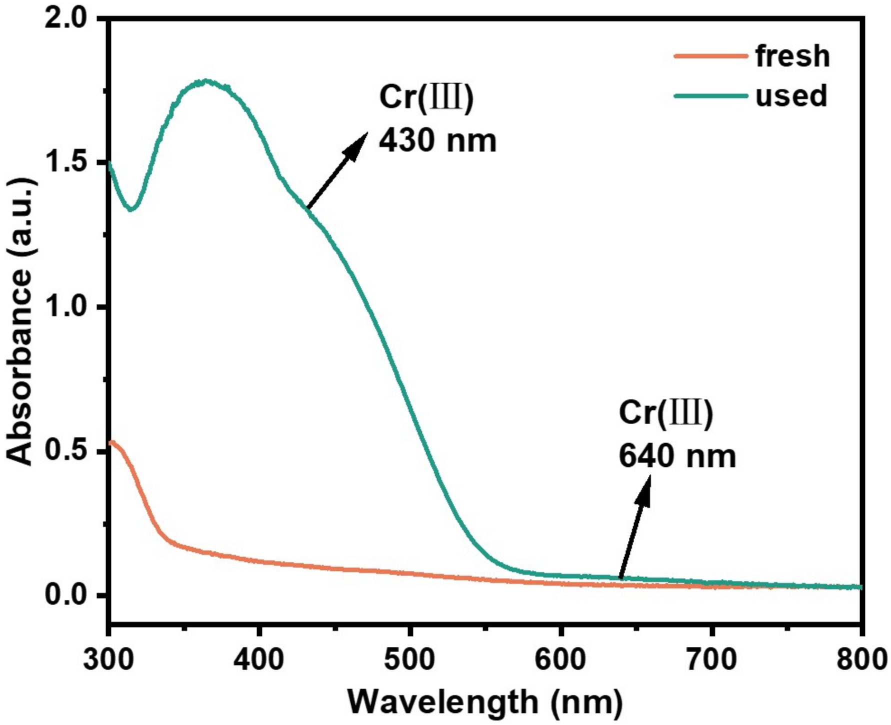

**Fig.** S16 UV-vis diffuse reflectance spectra of ZnAl-LDH-D before and after removal of $Cr^{VI}$.

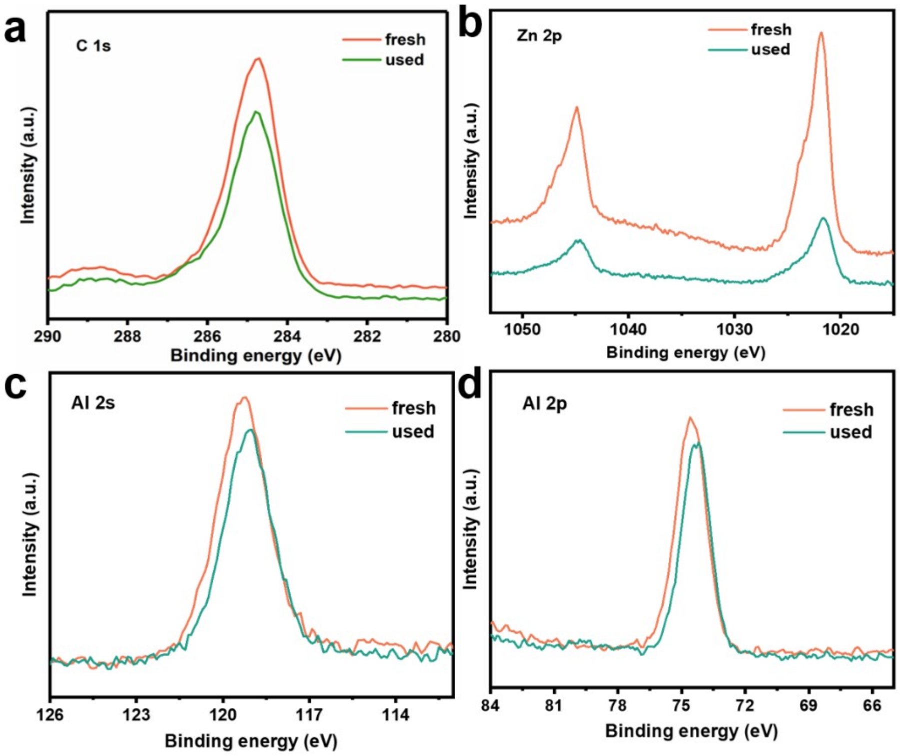

**Fig. S17** XPS of C1s, Zn2p, Al2s and Al2p binding energies in ZnAl-LDH-D before and after removal of $Cr^{VI}$.

**Table S1**. The removal performance of different adsorbent for $Cr^{VI}$.

| Adsorbents | Adsorption capacity（mg/g） | pH | Reaction time | Ref. |
|---|---|---|---|---|
| Zn Al-LDH-D | 73.4 | pH=4-10 | 1h | This work |
| LDH-EDTA | 47.62 | pH=3-10 | 2h | 1 |
| Zn-HC | 14 | pH=3 | 6h | 2 |
| Fh-Mn-5 | 48.5 | pH=9 | >24h | 3 |
| FPP | 21.55 | pH=2-10 | 0.17h | 4 |
| $MnO_2$/CS | 61.56 | pH=2 | 2h | 5 |
| NiCo-LDH | 99.9 | - | 1.5h | 6 |
| JTT | 10.99 | pH=3 | 0.5h | 7 |
| NMSH | 132.74 | pH=2-4 | 12h | 8 |

| | | | | |
|---|---|---|---|---|
| IOCs | 16.64–17.86 | pH=3 | 2h | 9 |
| Magnetic biocha | 77.5 | pH<6 | >24h | 10 |
| pBN-AS@MBA | 120.95 | pH=2 | 2h | 11 |
| ECAB-APTES-HCl | 53.19 | pH=2-9 | 4h | 12 |
| AC(activated carbon) | 180.01 | pH=2 | 12h | 13 |
| Polyacrylonitrile | 61.65 | - | 10h | 14 |

**Table S2**. Parameters of the Langmuir and Freundlich models.

| **Models** | Parameters | Temperature |
|---|---|---|
| | | 298K |
| **Langmuir** | Qmax (mg/g) | 69.49 |
| | $K_L$ (L/mg) | 2.97 |
| | $R^2$ | 0.99987 |
| **Freundlich** | $K_F$ | 41.55 |
| | n | 6.9 |
| | $R^2$ | 0.65058 |

**Table S3**. Kinetic model parameters for the adsorption of $Cr^{VI}$ on ZnAl-LDH-D

| **Models** | Parameters | Concentration (mg/L) |
|---|---|---|
| | | 50 |
| **Pseudo-first-order** | qe (mg/g) model | 28.00 |
| | $K_1$ ($h^{-1}$) | 0.05037 |
| | $R^2$ | 0.96159 |
| **Pseudo-second-order** | qe (mg/g) model | 51.98 |
| | qe (mg/g) experiment | 49.60 |
| | $K_2$ (g/m gh) | 0.00471 |
| | $R^2$ | 0.99997 |

## References:

1. Li J, Yan L, Yang Y, et al. Insight into the adsorption mechanisms of aqueous hexavalent chromium by EDTA intercalated layered double hydroxides: XRD, FTIR, XPS, and zeta potential studies. *New Journal of Chemistry*, 2019, 43(40): 15915-15923.

2. Li F, Zimmerman A R, Hu X, et al. Removal of aqueous Cr (VI) by Zn-and Al-modified hydrochar. *Chemosphere,* 2020, 260: 127610.

3. Liang C, Fu F, Tang B. Mn-incorporated ferrihydrite for Cr (VI) immobilization: Adsorption behavior and the fate of Cr (VI) during aging. *Journal of Hazardous Materials*, 2021, 417: 126073.

4. Wang Q, Zhou C, Kuang Y, et al. Removal of hexavalent chromium in aquatic solutions by pomelo peel. *Water Science and Engineering*, 2020, 13(1): 65-73.

5. Dinh V P, Nguyen M D, Nguyen Q H, et al. Chitosan-$MnO_2$ nanocomposite for effective removal of Cr (VI) from aqueous solution. *Chemosphere*, 2020, 257: 127147.

6. Hu H, Liu J, Xu Z, et al. Hierarchical porous Ni/Co-LDH hollow dodecahedron with excellent adsorption property for Congo red and Cr (VI) ions. Applied Surface Science, 2019, 478: 981-990.

7. Picazo-Rodríguez N G, Carrillo-Pedroza F R, Soria-Aguilar M J, et al. Use of Thermally Modified Jarosite for the Removal of Hexavalent Chromium by Adsorption. *Crystals*, 2022, 12(1): 80.

8. Deng J, Li X, Wei X, et al. Different adsorption behaviors and mechanisms of a novel amino-functionalized hydrothermal biochar for hexavalent chromium and pentavalent antimony. *Bioresource Technology,* 2020, 310: 123438.

9. Rathnayake S I, Martens W N, Xi Y, et al. Remediation of Cr (VI) by inorganic-organic clay.

*Journal of colloid and interface science*, 2017, 490: 163-173.

10. Han Y, Cao X, Ouyang X, et al. Adsorption kinetics of magnetic biochar derived from peanut hull on removal of Cr (VI) from aqueous solution: effects of production conditions and particle size. *Chemosphere*, 2016, 145: 336-341.

11. Song Z, Guo K, Bai W, et al. Adsorption and removal of Cr (VI) from aqueous solution with amine-functionalized porous boron nitride. *Journal of Solid State Chemistry*, 2022: 123720.

12. Fotsing P N, Bouazizi N, Woumfo E D, et al. Investigation of chromate and nitrate removal by adsorption at the surface of an amine-modified cocoa shell adsorbent. *Journal of Environmental Chemical Engineering*, 2021, 9(1): 104618.

13. Zeng H, Zeng H, Zhang H, et al. Efficient adsorption of Cr (VI) from aqueous environments by phosphoric acid activated eucalyptus biochar. *Journal of Cleaner Production*, 2021, 286: 124964.

14. Yang X, Zhou Y, Sun Z, et al. Synthesis and Cr adsorption of a super-hydrophilic polydopamine-functionalized electrospun polyacrylonitrile. *Environmental Chemistry Letters*, 2021, 19(1): 743-749.